

# Higgs Precision at FCC-ee

Jae Sik Lee (Chonnam Nat'l Univ.)

**K-FCC Brainstorming Workshop** 12-14 November 2021, Gyeongju

Main Ref.: *FCC Physics Opportunities* Eur. Phys. J. C (2019) 79:474

Future Circular Collider Conceptual Design Report Volume 1

- **The first-phase LHC legacy:**
  - (a) the discovery of the Higgs boson
  - (b) the indication that signals of new physics around the TeV scale are, at best, elusive
  - (c) the rapid advance of theoretical calculations: precision measurements, from the Higgs to the flavour sectors
  - (d) the extraordinary achievements of the accelerator and of the detectors

영어 ↔ 한국어

the indication that signals of new physics around the TeV scale are, at best, elusive

TeV 규모 주변의 새로운 물리학 신호가 기껏해야 파악하기 어렵다는 표시

TeV gyumo jubyeon-ui saeloun mullihag sinhoga gikkeoshaeya paaghagi eolyeobdaneun pyosi

Google 번역에서 열기 • 사용자 의견

Beginning of the end? Too early to despair... *J.Song*

- FCC CDR I (EPJC2019) wrote:

“After 10 years of physics at the Large Hadron Collider, the particle physics landscape has greatly evolved. The proposed lepton collider **FCC-ee** is a *high-precision instrument to study the Z, W, Higgs and top particles, and offers great direct and indirect sensitivity to new physics*. Most of the FCC-ee infrastructure could be reused for a subsequent hadron collider **FCC-hh**. The latter would provide proton–proton collisions at a centre-of-mass energy of 100 TeV and directly produce new particles with masses of up to several tens of TeV. It will also measure the Higgs self-coupling with unprecedented precision. **Heavy-ion collisions** and **ep collisions** would contribute to the breadth of the overall FCC programme.”

⇒ Higgs\_Precision@FCC-ee

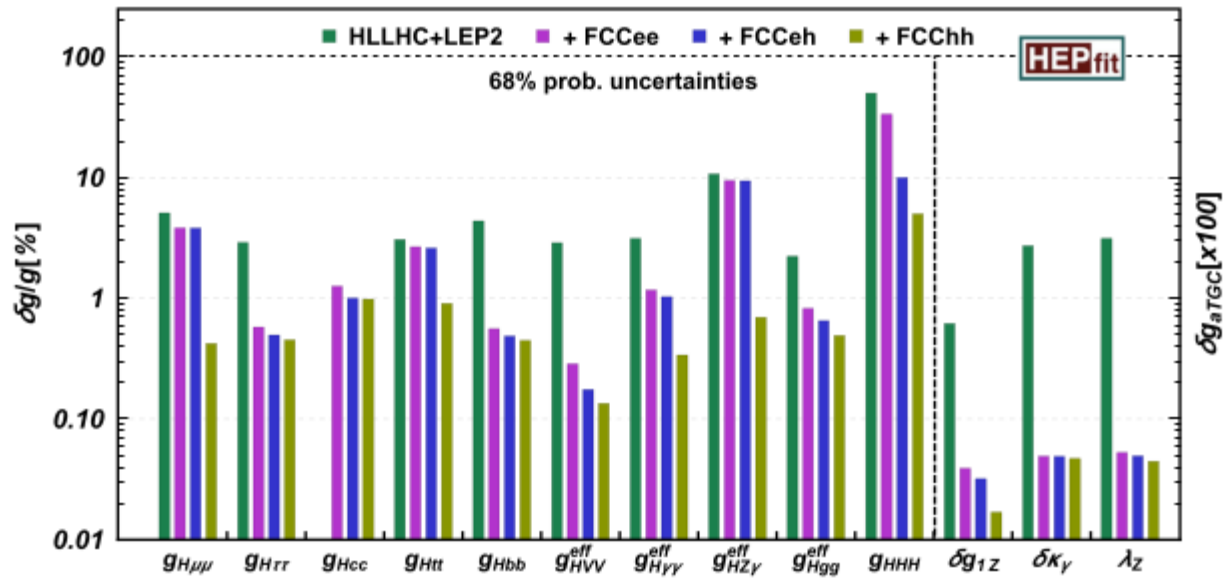


**Fig. S.1** One- $\sigma$  precision reach at the FCC on the effective single Higgs couplings, Higgs self-coupling, and anomalous triple gauge couplings in the EFT framework. Absolute precision in the EW measurements is assumed. The different bars illustrate the improvements that

would be possible by combining each FCC stage with the previous knowledge at that time (precisions at each FCC stage considered individually, reported in Tables S.1 and S.2 in the  $\kappa$  framework, are quite different)

2. 이재식 교수님: FCC-ee (CEPC 예도 해당) 에서 예상 되는 Higgs precision 과 그에 따른 물리적 의미를 전달.

예로서 ...

- 테이블에 여러 coupling들의 projection 이 있는데 .. 이 모든 것들이 다 중요한 것인지, 어떤 특정한 coupling의 정밀도 측정이 더 중요한 것인지에 대해 물리적으로 설명. 예로서 H-Z 상수가 0.1% 정도로 측정된다고 했을때 이 것이 의미하는 물리적 의미를 EFT 의 unitarity violation 관점에서 또는 future Higgs precision measurement 관점에서 (교수님께서 말씀하셨듯이, H-Z 는 input 으로 가정하고 다른 상수들을 측정 etc), 또는 다른 중요한 물리적 관점에서 설명?

- FCC-ee 나 CEPC 없이 바로 FCC-hh로 가면 상황이 어떻게 될까? (즉, FCC-ee, CEPC에서 예상하는 Higgs precision 이 달성되지 않는다면 FCC-hh 의 상황은 어떻게 될런지 ...)

# • FCC\_ee

The future circular collider, **FCC**, hosted in a 100 km tunnel, builds on this legacy, and on the experience of previous circular colliders (LEP, HERA and the Tevatron). The  $e^+e^-$  collider (FCC-ee) would operate at multiple centre of mass energies  $\sqrt{s}$ , producing  $5 \times 10^{12}$   $Z^0$  bosons ( $\sqrt{s} \sim 91$  GeV),  $10^8$  WW pairs ( $\sqrt{s} \sim 160$  GeV), over  $10^6$  Higgses ( $\sqrt{s} \sim 240$  GeV), and over  $10^6$   $t\bar{t}$  pairs ( $\sqrt{s} \sim 350$ – $365$  GeV). The 100 TeV pp collider (FCC-hh) is designed to collect a total luminosity of  $20 \text{ ab}^{-1}$ , corresponding to the production of e.g. more than  $10^{10}$  Higgs bosons produced. FCC-hh can also be operated with heavy ions (e.g. PbPb at  $\sqrt{s_{NN}} = 39$  TeV). Optionally, the FCC-eh, with 50 TeV proton beams colliding with 60 GeV electrons from an energy-recovery linac, would generate  $\sim 2 \text{ ab}^{-1}$  of 3.5 TeV ep collisions.

## $10^6 e^+ e^- \rightarrow HZ$ (5/ab, 3years)

**Fig. 4.1** The Higgs boson production cross section as a function of the centre-of-mass energy in unpolarised  $e^+e^-$  collisions. The blue and green curves stand for the Higgsstrahlung and WW fusion processes, respectively, and the red curve displays the total production cross section. The vertical dotted lines indicate the centre-of-mass energies of choice at the FCC-ee for the measurement of the Higgs boson properties

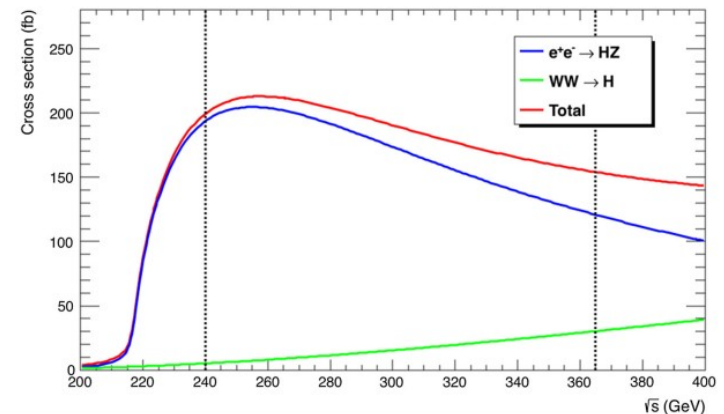


**Table S.1** Precisions determined in the  $\kappa$  framework on the Higgs boson couplings and total decay width, as expected from the FCC-ee data, and compared to those from HL-LHC. All numbers indicate 68% C.L. sensitivities, except for the last line which gives the 95% C.L. sensitivity on the “exotic” branching fraction, accounting for final states that cannot be tagged as SM decays. The fit to the HL-LHC projections alone (first column) requires assumptions: here, the branching ratios into  $c\bar{c}$  and into exotic particles (and those not indicated in the table)

are set to their SM values. The FCC-ee accuracies are subdivided in three categories: the first sub-column gives the results of the fit expected with  $5 \text{ ab}^{-1}$  at 240 GeV, the second sub-column in bold includes the additional  $1.5 \text{ ab}^{-1}$  at  $\sqrt{s} = 365 \text{ GeV}$ , and the last sub-column shows the result of the combined fit with HL-LHC. Similar to the HL-LHC, the fit to the FCC-ee projections alone requires an assumption to be made: here the total width is set to its SM value, but in practice will be taken to be the value measured by the FCC-ee

Collider	HL-LHC	ILC <sub>250</sub>	CLIC <sub>380</sub>	FCC-ee			FCC-eh
Luminosity ( $\text{ab}^{-1}$ )	3	2	0.5	5 @ 240 GeV	+ 1.5 @ 365 GeV	+ HL-LHC	2
Years	25	<b>15</b>	8	<b>3</b>	+ 4	–	20
$\delta\Gamma_H / \Gamma_H$ (%)	<b>SM</b>	3.6	4.7	<b>2.7</b>	<b>1.3</b>	1.1	SM
$\delta g_{HZZ} / g_{HZZ}$ (%)	1.5	0.30	0.60	<b>0.2</b>	<b>0.17</b>	0.16	0.43
$\delta g_{HWW} / g_{HWW}$ (%)	1.7	1.7	1.0	1.3	<b>0.43</b>	0.40	0.26
$\delta g_{Hbb} / g_{Hbb}$ (%)	3.7	1.7	2.1	1.3	<b>0.61</b>	0.56	0.74
$\delta g_{Hcc} / g_{Hcc}$ (%)	<b>SM</b>	2.3	4.4	1.7	<b>1.21</b>	1.18	1.35
$\delta g_{Hgg} / g_{Hgg}$ (%)	2.5	2.2	2.6	1.6	<b>1.01</b>	<b>0.90</b>	1.17
$\delta g_{H\tau\tau} / g_{H\tau\tau}$ (%)	1.9	1.9	3.1	1.4	<b>0.74</b>	0.67	1.10
$\delta g_{H\mu\mu} / g_{H\mu\mu}$ (%)	4.3	14.1	n.a.	10.1	<b>9.0</b>	3.8	n.a.
$\delta g_{H\gamma\gamma} / g_{H\gamma\gamma}$ (%)	1.8	6.4	n.a.	4.8	<b>3.9</b>	<b>1.3</b>	2.3
$\delta g_{Htt} / g_{Htt}$ (%)	3.4	–	–	–	–	3.1	1.7
BR <sub>EXO</sub> (%)	<b>SM</b>	< 1.8	< 3.0	< 1.2	< <b>1.0</b>	< 1.0	n.a.

The FCC-ee will also provide a first measurement of the Higgs self-coupling to 32%.

- Absolute measurement of the Higgs couplings to Z and Gamma\_H: a starting point for the Higgs\_precision@FCC-ee!

improved analysis that exploits the superior performance of the CLD detector design (see the FCC-ee CDR, Sect. 7). The total Higgs production cross section is determined by counting  $e^+e^- \rightarrow HZ$  events tagged with a leptonic Z decay,  $Z \rightarrow \ell^+\ell^-$ , independently of the Higgs boson decay. An example of such an event is displayed in Fig. 4.2 (left). The mass  $m_{\text{Recoil}}$  of the

474 Page 46 of 161

Eur. Phys. J. C (2019) 79:474

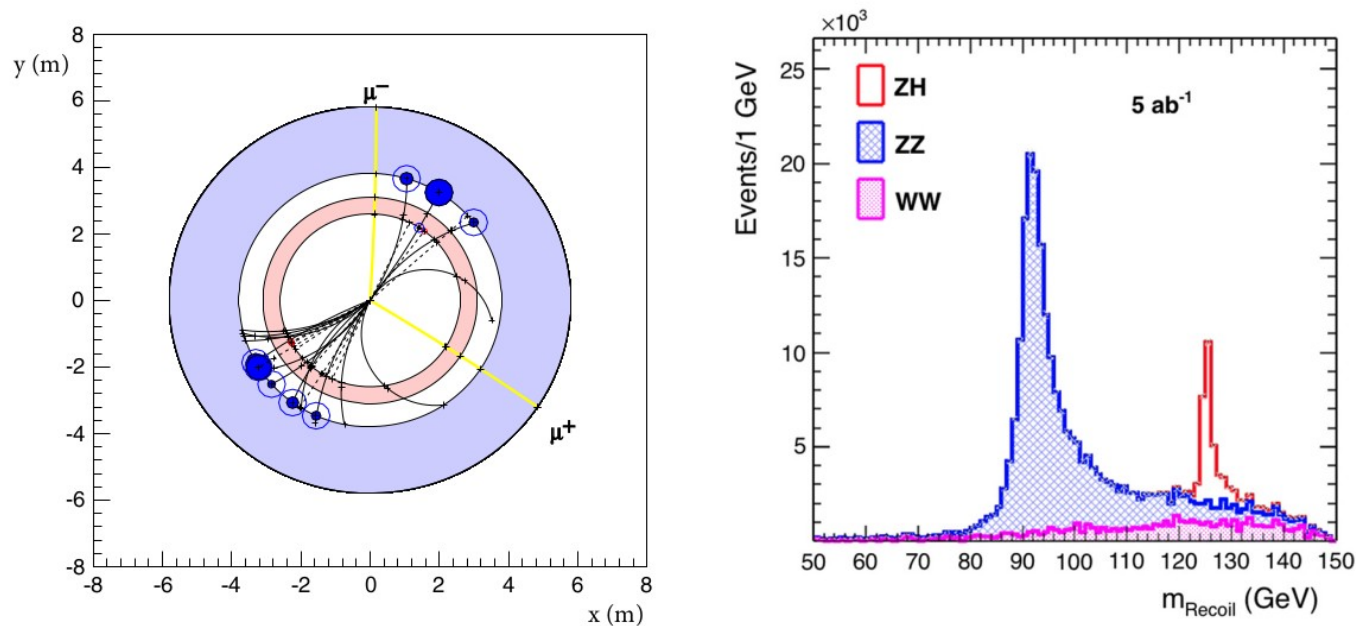


**Fig. 4.2** Left: a schematic view, transverse to the detector axis, of an  $e^+e^- \rightarrow HZ$  event with  $Z \rightarrow \mu^+\mu^-$  and with the Higgs boson decaying hadronically. The two muons from the Z decay are indicated. Right: distribution of the mass recoiling against the muon pair, determined

from the total energy-momentum conservation, with an integrated luminosity of  $5 \text{ ab}^{-1}$  and the CLD detector design. The peak around 125 GeV (in red) consists of HZ events. The rest of the distribution (in blue and pink) originate from ZZ and WW production

to the ratio  $\sigma_{HZ} \times \Gamma(H \rightarrow ZZ)/\Gamma_H$ , hence to  $g_{HZZ}^2/\Gamma_H$ . The measurement of  $g_{HZZ}$  described above thus allows  $\Gamma_H$  to be extracted. The numbers of events with exclusive decays of the Higgs boson into  $b\bar{b}$ ,  $c\bar{c}$ ,  $gg$ ,  $\tau^+\tau^-$ ,  $\mu^+\mu^-$ ,  $W^+W^-$ ,  $\gamma\gamma$ ,  $Z\gamma$ ,



# • Higgs signal strengths@LHC

## 5.1. Higgs signal strengths

Each theoretical signal strength can be written in a product form as

$$\widehat{\mu}(\mathcal{P}, \mathcal{D}) \simeq \widehat{\mu}(\mathcal{P}) \widehat{\mu}(\mathcal{D}), \quad (176)$$

where  $\mathcal{P} = \text{ggF}, \text{VBF}, \text{VH}, \text{ttH}$  denote the production mechanisms and  $\mathcal{D} = \gamma\gamma, ZZ^{(*)}, WW^{(*)}, b\bar{b}, \tau^+\tau^-$  the decay channels, which are experimentally clean and/or dominant for  $M_H \simeq 125$  GeV. The factorization assumption is valid only when the production and decay processes are well separated like as in the resonant  $s$ -channel Higgs production in the NWA. By factorizing them, non-resonant and interference effects are inevitably neglected. More explicitly, at LO, the production signal strengths are given in terms of the relevant form factors and couplings by

$$\begin{aligned} \widehat{\mu}(\text{ggF}) &= \frac{|S^g(M_H)|^2 + |P^g(M_H)|^2}{|S_{\text{SM}}^g(M_H)|^2}, \\ \widehat{\mu}(\text{VBF}) &= \widehat{\mu}(\text{VH}) = g_{HWW, HZZ}^2, \\ \widehat{\mu}(\text{ttH}) &= (g_{H\bar{t}t}^S)^2 + (g_{H\bar{t}t}^P)^2, \end{aligned} \quad (177)$$

and the decay signal strengths by

$$\widehat{\mu}(\mathcal{D}) = \frac{B(H \rightarrow \mathcal{D})}{B(H_{\text{SM}} \rightarrow \mathcal{D})}, \quad (178)$$

with the branching fraction of each decay mode defined by

$$B(H \rightarrow \mathcal{D}) = \frac{\Gamma(H \rightarrow \mathcal{D})}{\Gamma_{\text{tot}}(H) + \Delta\Gamma_{\text{tot}}}. \quad (179)$$

Note that an arbitrary non-SM contribution  $\Delta\Gamma_{\text{tot}}$  to the total decay width is introduced. We observe  $\Gamma_{\text{tot}}(H)$  becomes the SM total decay width when  $g_{H\bar{f}f}^S = 1$ ,  $g_{H\bar{f}f}^P = 0$ ,  $g_{HWW, HZZ} = 1$ , and  $\Delta S^{\gamma, g, Z\gamma} = \Delta P^{\gamma, g, Z\gamma} = 0$ . Note that the LO relations in Eq. (177) are most reliable when higher order corrections to a BSM production cross section and those to the corresponding SM one are the same and so they are canceled out in the BSM-to-SM ratios. Otherwise they are valid at LO strictly.

- $g_{\text{HZZ}} / g^{\text{SM}}_{\text{HZZ}} < 1$  indicates the existence of additional Higgs bosons participating in EWSB:

$$g^2 \sim 1 - (Z_6 v^2 / M_{\text{Heavy}})^2 \quad [2\text{HDM}]$$

- EWPT (FCC-hh ... *M.Son*)

$$\begin{aligned}
 V_{\mathcal{H}} = & Y_1(\mathcal{H}_1^\dagger \mathcal{H}_1) + Y_2(\mathcal{H}_2^\dagger \mathcal{H}_2) + Y_3(\mathcal{H}_1^\dagger \mathcal{H}_2) + Y_3^*(\mathcal{H}_2^\dagger \mathcal{H}_1) \\
 & + Z_1(\mathcal{H}_1^\dagger \mathcal{H}_1)^2 + Z_2(\mathcal{H}_2^\dagger \mathcal{H}_2)^2 + Z_3(\mathcal{H}_1^\dagger \mathcal{H}_1)(\mathcal{H}_2^\dagger \mathcal{H}_2) + Z_4(\mathcal{H}_1^\dagger \mathcal{H}_2)(\mathcal{H}_2^\dagger \mathcal{H}_1) \\
 & + Z_5(\mathcal{H}_1^\dagger \mathcal{H}_2)^2 + Z_5^*(\mathcal{H}_2^\dagger \mathcal{H}_1)^2 + Z_6(\mathcal{H}_1^\dagger \mathcal{H}_1)(\mathcal{H}_1^\dagger \mathcal{H}_2) + Z_6^*(\mathcal{H}_1^\dagger \mathcal{H}_1)(\mathcal{H}_2^\dagger \mathcal{H}_1) \\
 & + Z_7(\mathcal{H}_2^\dagger \mathcal{H}_2)(\mathcal{H}_1^\dagger \mathcal{H}_2) + Z_7^*(\mathcal{H}_2^\dagger \mathcal{H}_2)(\mathcal{H}_2^\dagger \mathcal{H}_1),
 \end{aligned}$$

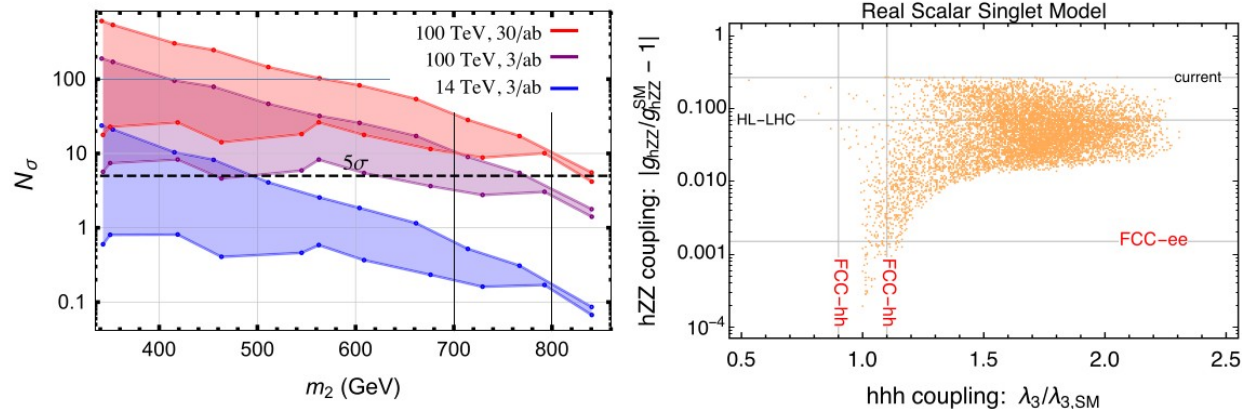


**Fig. S.3** Manifestations of models with a singlet-induced strong first order EWPT. Left: discovery potential at HL-LHC and FCC-hh, for the resonant di-Higgs production, as a function of the singlet-like scalar mass  $m_2$ .  $4\tau$  and  $b\bar{b}\gamma\gamma$  final states are combined. Right: correlation

between changes in the HZZ coupling (vertical axis) and the HHH coupling scaled to its SM value (horizontal axis), in a scan of the models' parameter space. All points give rise to a first order phase transition

# • Higgs precisions@FCC-ee(repeat)

**Table S.1** Precisions determined in the  $\kappa$  framework on the Higgs boson couplings and total decay width, as expected from the FCC-ee data, and compared to those from HL-LHC. All numbers indicate 68% C.L. sensitivities, except for the last line which gives the 95% C.L. sensitivity on the “exotic” branching fraction, accounting for final states that cannot be tagged as SM decays. The fit to the HL-LHC projections alone (first column) requires assumptions: here, the branching ratios into  $c\bar{c}$  and into exotic particles (and those not indicated in the table)

are set to their SM values. The FCC-ee accuracies are subdivided in three categories: the first sub-column gives the results of the fit expected with  $5 \text{ ab}^{-1}$  at 240 GeV, the second sub-column in bold includes the additional  $1.5 \text{ ab}^{-1}$  at  $\sqrt{s} = 365 \text{ GeV}$ , and the last sub-column shows the result of the combined fit with HL-LHC. Similar to the HL-LHC, the fit to the FCC-ee projections alone requires an assumption to be made: here the total width is set to its SM value, but in practice will be taken to be the value measured by the FCC-ee

Collider	HL-LHC	ILC <sub>250</sub>	CLIC <sub>380</sub>	FCC-ee			FCC-eh
Luminosity ( $\text{ab}^{-1}$ )	3	2	0.5	5 @ 240 GeV	+ 1.5 @ 365 GeV	+ HL-LHC	2
Years	25	<b>15</b>	8	<b>3</b>	+ 4	–	20
$\delta\Gamma_{\text{H}}/\Gamma_{\text{H}}$ (%)	<b>SM</b>	3.6	4.7	<b>2.7</b>	<b>1.3</b>	1.1	SM
$\delta g_{\text{HZZ}}/g_{\text{HZZ}}$ (%)	1.5	0.30	0.60	<b>0.2</b>	<b>0.17</b>	0.16	0.43
$\delta g_{\text{HWW}}/g_{\text{HWW}}$ (%)	1.7	1.7	1.0	1.3	<b>0.43</b>	0.40	0.26
$\delta g_{\text{Hbb}}/g_{\text{Hbb}}$ (%)	3.7	1.7	2.1	1.3	<b>0.61</b>	0.56	0.74
$\delta g_{\text{Hcc}}/g_{\text{Hcc}}$ (%)	<b>SM</b>	2.3	4.4	1.7	<b>1.21</b>	1.18	1.35
$\delta g_{\text{Hgg}}/g_{\text{Hgg}}$ (%)	2.5	2.2	2.6	1.6	<b>1.01</b>	<b>0.90</b>	1.17
$\delta g_{\text{H}\tau\tau}/g_{\text{H}\tau\tau}$ (%)	1.9	1.9	3.1	1.4	<b>0.74</b>	0.67	1.10
$\delta g_{\text{H}\mu\mu}/g_{\text{H}\mu\mu}$ (%)	4.3	14.1	n.a.	10.1	<b>9.0</b>	3.8	n.a.
$\delta g_{\text{H}\gamma\gamma}/g_{\text{H}\gamma\gamma}$ (%)	1.8	6.4	n.a.	4.8	<b>3.9</b>	<b>1.3</b>	2.3
$\delta g_{\text{Ht}}/g_{\text{Ht}}$ (%)	3.4	–	–	–	–	3.1	1.7
BR <sub>EXO</sub> (%)	<b>SM</b>	< 1.8	< 3.0	< 1.2	< <b>1.0</b>	< 1.0	n.a.

- $dg_{Hgg}/g_{Hgg} \sim 1\%$

S.Y. Choi, J.S. Lee and J. Park

Progress in Particle and Nuclear Physics 120 (2021) 103880

**Table 11**  
(CPC) The best-fitted values in various CP conserving fits and the corresponding  $\chi^2$  per degree of freedom (*dof*) and goodness of fit. The *p*-value for each fit hypothesis against the SM null hypothesis is also shown. For the SM, we obtain  $\chi^2 = 53.81$ ,  $\chi^2/dof = 53.81/64$ , and so the goodness of fit = 0.814. From Ref. [258].

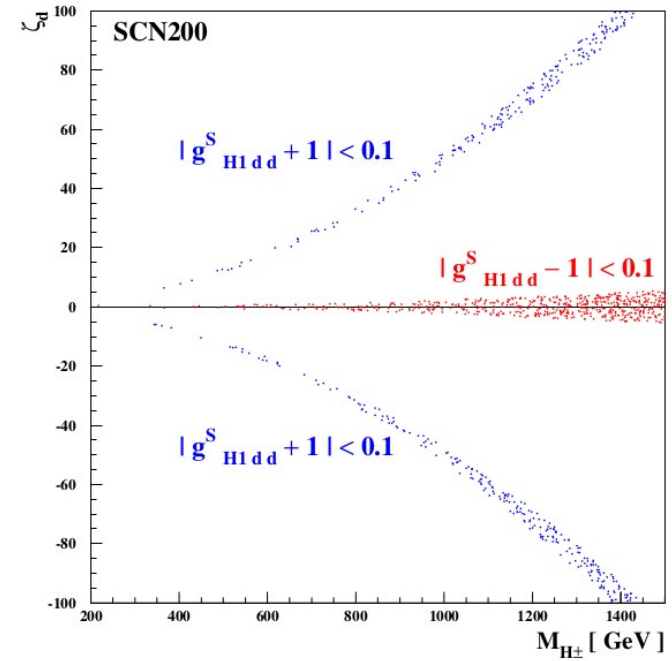
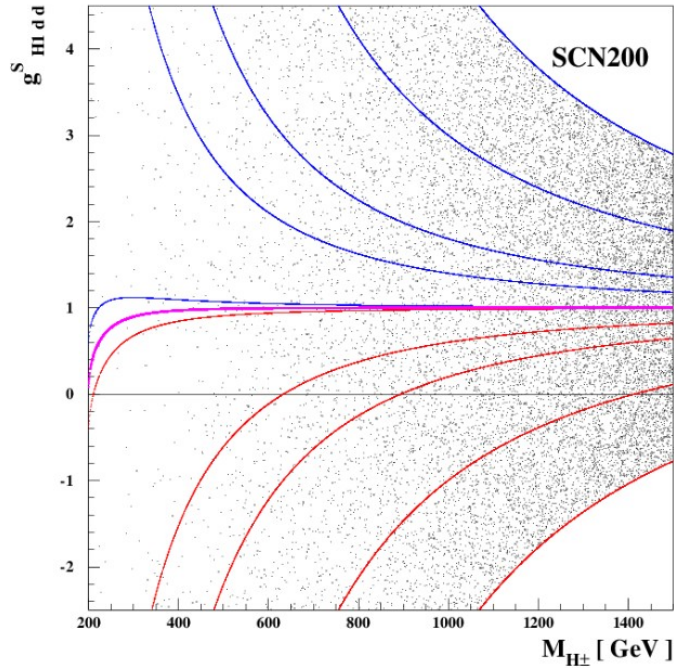
Cases	CPC1	CPC2	CPC4	CPCN4			
Varying Parameters	$\Delta\Gamma_{\text{tot}}$	$\Delta S^\gamma$ $\Delta S^g$	$C_u^S, C_d^S,$ $C_\ell^S, C_\nu$	$C_u^S, C_\nu$ $\Delta S^\gamma, \Delta S^g$			
$C_u^S$	1	1	$1.001^{+0.056}_{-0.055}$	$1.042^{+0.077}_{-0.081}$	$1.042^{+0.078}_{-0.081}$	$-1.042^{+0.081}_{-0.078}$	$-1.042^{+0.081}_{-0.078}$
$C_d^S$	1	1	$0.962^{+0.101}_{-0.101}$	1	1	1	1
$C_\ell^S$	1	1	$1.024^{+0.093}_{-0.093}$	1	1	1	1
$C_\nu$	1	1	$1.019^{+0.044}_{-0.045}$	$1.027^{+0.034}_{-0.036}$	$1.027^{+0.034}_{-0.036}$	$1.028^{+0.034}_{-0.036}$	$1.028^{+0.034}_{-0.036}$
$\Delta S^\gamma$	0	$-0.226^{+0.32}_{-0.32}$	0	$-0.129^{+0.37}_{-0.37}$	$-0.129^{+0.37}_{-0.37}$	$3.524^{+0.41}_{-0.42}$	$3.523^{+0.41}_{-0.42}$
$\Delta S^g$	0	$0.016^{+0.025}_{-0.025}$	0	$-0.021^{+0.057}_{-0.055}$	$-1.34^{+0.066}_{-0.065}$	$0.095^{+0.055}_{-0.057}$	$1.414^{+0.066}_{-0.066}$
$\Delta\Gamma_{\text{tot}}$ (MeV)	$-0.285^{+0.18}_{-0.17}$	0	0	0	0	0	0
$\chi^2/dof$	51.44/63	51.87/62	50.79/60	50.96/60			
Goodness of fit	0.851	0.817	0.796	0.791			
<i>p</i> -value	0.124	0.379	0.554	0.583			

For the decay  $H \rightarrow gg$ , the scalar and pseudoscalar form factors and the relevant radiative corrections are given numerically apart from the scalar and pseudoscalar Higgs–fermion–fermion couplings by

$$\begin{aligned}
 S^g &= 0.688 g_{H\bar{t}t}^S + (-0.043 + 0.062i) g_{H\bar{b}b}^S + (-0.009 + 0.008i) g_{H\bar{c}c}^S + \Delta S^g; \\
 P^g &= 1.048 g_{H\bar{t}t}^P + (-0.049 + 0.063i) g_{H\bar{b}b}^P + (-0.010 + 0.008i) g_{H\bar{c}c}^P + \Delta P^g; \\
 \delta_{\text{QCD}}^{g:S} &= 0.8850, \quad \delta_{\text{elw}}^{g:S} = 0.0516; \quad \delta_{\text{QCD}}^{g:P} = 0.8775, \quad \delta_{\text{elw}}^{g:P} = -0.0218,
 \end{aligned} \tag{153}$$

where  $\delta_{\text{elw}}^{g:S}$  is from Fig. 9 and we set  $\eta_{\text{elw}}^{g:P} = 0$  for  $\delta_{\text{elw}}^{g:P}$ . In the SM, we have  $S^g = 0.636 + 0.070i$  and  $P^g = 0$ . Similarly

- Wrong-sign  $H_1$  coupling might imply large heavy Higgs Yukawa couplings 13



S.Y.Choi, JSL, J.Park, e-Print: 2110.03908 [hep-ph]

$$-\mathcal{L}_{H_i \bar{f} f} = \sum_{i=1}^3 \sum_{f=u,d,c,s,t,b,e,\mu,\tau} \frac{m_f}{v} \bar{f} \left( g_{H_i \bar{f} f}^S + i g_{H_i \bar{f} f}^P \gamma_5 \right) f H_i \quad (49)$$

with the scalar and pseudoscalar couplings given by

$$\begin{aligned} g_{H_i \bar{f} f}^S &= O_{\varphi_1 i} + \Re(\zeta_f) O_{\varphi_2 i} \pm \Im(\zeta_f) O_{a i}, \\ g_{H_i \bar{f} f}^P &= \Im(\zeta_f) O_{\varphi_2 i} \mp \Re(\zeta_f) O_{a i}, \end{aligned} \quad (50)$$

where the upper and lower signs are for the up-type fermions  $f = u, c, t$  and the down-type fermions  $f = d, s, b, e, \mu, \tau$ , respectively. The simultaneous existence of the scalar  $g_{H_i \bar{f} f}^S$  and pseudoscalar

- $dg_{Haa}/g_{Haa} \sim 1\%$

S.Y. Choi, J.S. Lee and J. Park

Progress in Particle and Nuclear Physics 120 (2021) 103880

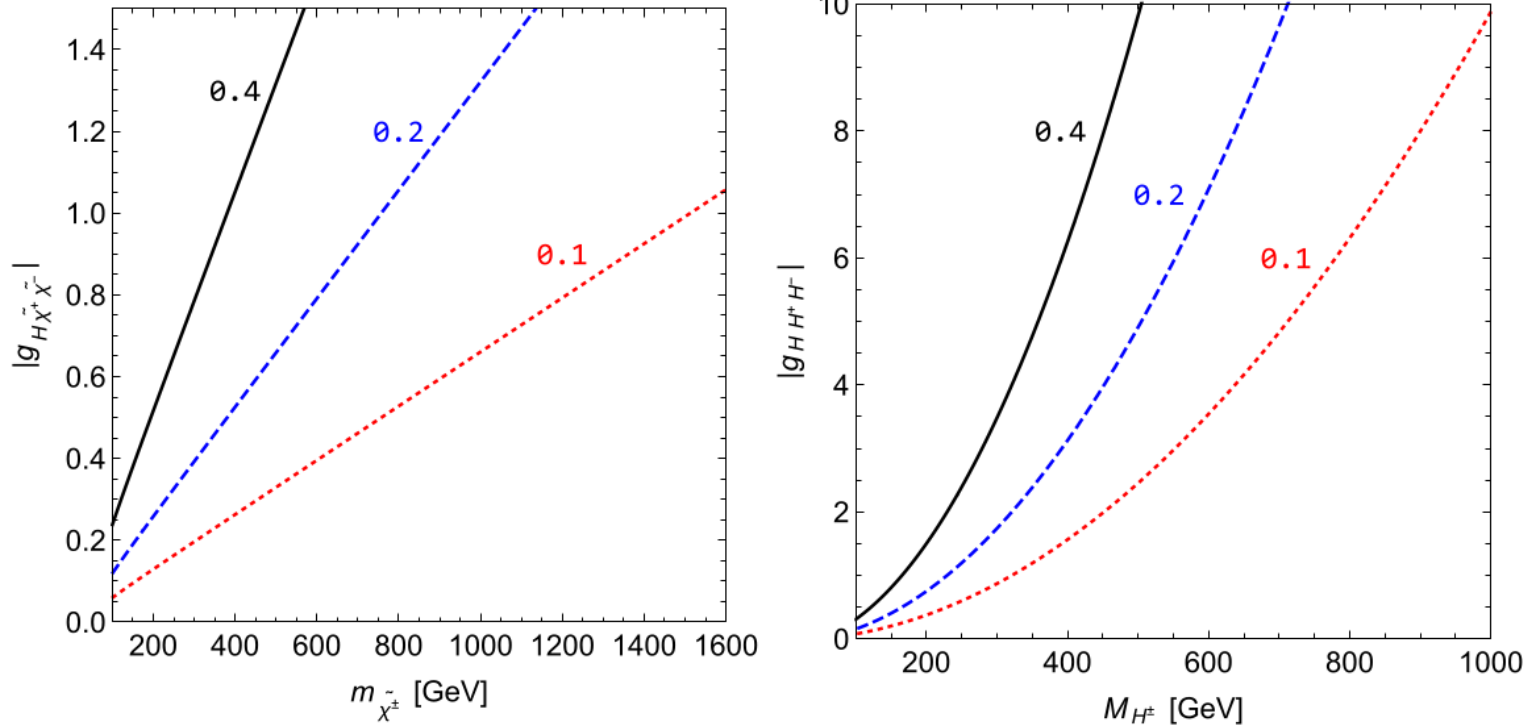


**Fig. 34.** (Left) Contour lines for  $|\Delta S^\gamma| = 0.4, 0.2, 0.1$  from left to right on the  $(m_{\tilde{\chi}_1^\pm}, |g_{H\tilde{\chi}_1^+\tilde{\chi}_1^-}|)$  plane assuming the lighter-chargino-loop contributions dominate  $\Delta S^\gamma$ . (Right) The same as in the left panel but on the  $(M_{H^\pm}, |g_{HH^+H^-}|)$  plane now assuming  $\Delta S^\gamma$  is dominated by the contributions from charged-Higgs loops. For the reference value of  $|\Delta S^\gamma| = 0.4$ , we are taking the  $1\sigma$  error of the **CPCN4** fit.

$$S^\gamma = -8.341 g_{HWW} + 1.826 g_{H\bar{t}t}^S + (-0.020 + 0.024 i) g_{H\bar{b}b}^S + (-0.023 + 0.021 i) g_{H\bar{\tau}\tau}^S + \Delta S^\gamma ;$$

In the SM, we have  $\bar{S}^\gamma = -\hat{6}.558 + 0.047 i$

- Summary : Higgs\_Precision@FCC-ee

In addition to the unique electroweak precision measurement programme presented earlier, the FCC-ee provides the best model-independent precisions for all couplings accessible from Higgs boson decays among the  $e^+e^-$  collider projects at the EW scale. With larger luminosities delivered to several detectors at several centre-of-mass energies (240, 350, and 365 GeV), the FCC-ee improves on the model-dependent HL-LHC precision by an order of magnitude for all non-rare decays, and is therefore able to test the Higgs boson at the one-loop level of the SM, without the need of a costly  $e^+e^-$  centre-of-mass energy upgrade. The FCC-ee also determines the Higgs boson width with a precision of 1.3%, which in turn allows the HL-LHC measurements to be interpreted in a model-independent way as well. Other  $e^+e^-$  colliders at the EW scale are limited by the precision with which the HZ or the WW fusion cross sections can be measured, i.e., by the luminosity delivered either at 240–250 GeV, or at 365–380 GeV, or both.

- Summary: whole FCC programme

**FCC-ee** dictates the ‘position’ of NP and then **FCC-hh** directly probes NP there equipped with precise PDFs from **FCC-eh**

D,W.Jung, P.Ko, JSL, e-Print: 1111.3180 [hep-ph] (PLB)

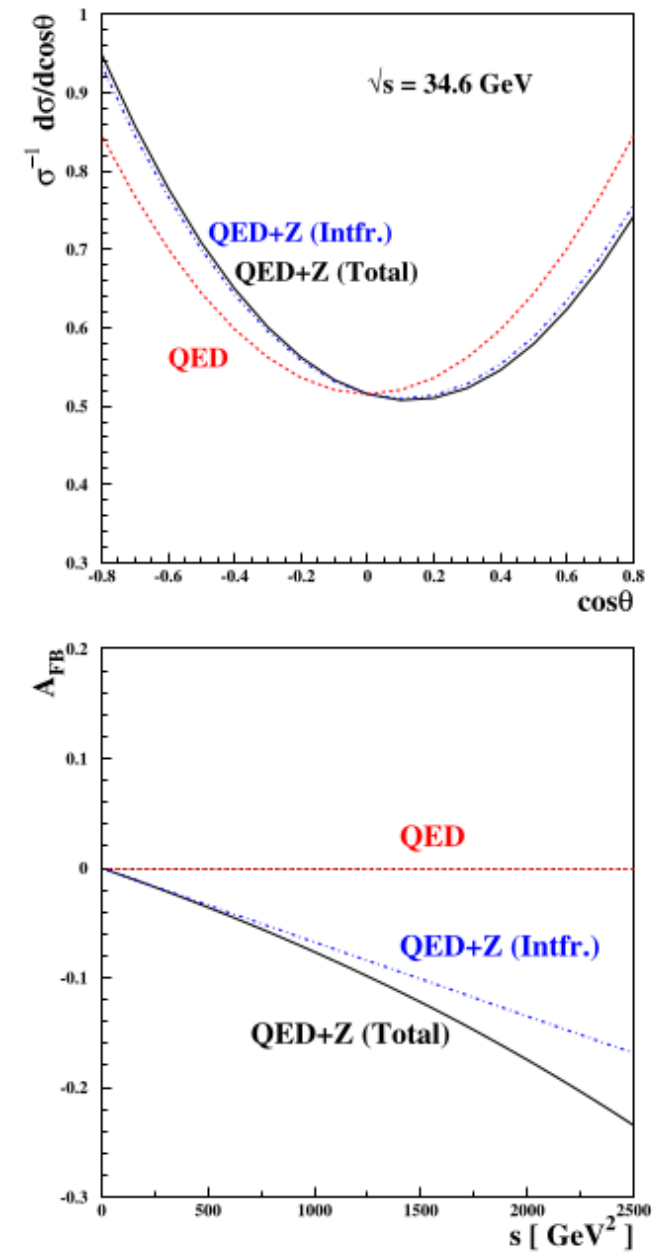


Fig. 1. (Upper) The normalized angular distribution of  $e^+e^- \rightarrow \mu^+\mu^-$  at PETRA ( $\sqrt{s} \simeq 34.6$  GeV), and (lower) the integrated  $A_{FB}$  as functions of  $s$  up to  $s = 2500$  GeV<sup>2</sup>. The dashed (red in the web version) curves are for the symmetric QED case. The dash-dotted (blue in the web version) curves include only the interference between the diagrams mediated by  $\gamma$  and  $Z^0$  bosons. The full QED + Z prediction is represented by the solid (black) curves.



**BACK UP**

# • Decay widths and Brs of the SM Higgs

S.Y. Choi, J.S. Lee and J. Park

Progress in Particle and Nuclear Physics 120 (2021) 103880

**Table 6**

Partial and total decay widths of the SM Higgs in MeV taking  $M_H = 125.5$  GeV. We compare our numerical estimates with those presented in Ref. [84] by introducing a quantity  $\delta_r$  defined by  $\delta_r \equiv (\Gamma_{\text{This Review}} - \Gamma_{\text{Ref. [84]}}) / \Gamma_{\text{Ref. [84]}}$ . Also presented are theoretical uncertainties (THUs) of the partial and total decay widths from missing higher orders estimated around  $M_H = 125$  GeV, see Tables 178 and 182 in Ref. [84].

	$\Gamma(H \rightarrow b\bar{b})$	$\Gamma(H \rightarrow WW)$	$\Gamma(H \rightarrow gg)$	$\Gamma(H \rightarrow \tau\tau)$	$\Gamma(H \rightarrow c\bar{c})$
This Review	2.367	$9.185 \times 10^{-1}$	$3.382 \times 10^{-1}$	$2.572 \times 10^{-1}$	$1.173 \times 10^{-1}$
Ref. [84]	2.387	$9.222 \times 10^{-1}$	$3.386 \times 10^{-1}$	$2.573 \times 10^{-1}$	$1.185 \times 10^{-1}$
$\delta_r$ [%]	-0.8	-0.4	-0.1	-0.05	-1.0
THU [%]	$\pm 0.5$	$\pm 0.5$	$\pm 3.2$	$\pm 0.5$	$\pm 0.5$
	$\Gamma(H \rightarrow ZZ)$	$\Gamma(H \rightarrow \gamma\gamma)$	$\Gamma(H \rightarrow Z\gamma)$	$\Gamma(H \rightarrow \mu\mu)$	$\Gamma_{\text{tot}}$
This Review	$1.139 \times 10^{-1}$	$9.405 \times 10^{-3}$	$6.531 \times 10^{-3}$	$8.913 \times 10^{-4}$	4.129
Ref. [84]	$1.139 \times 10^{-1}$	$9.438 \times 10^{-3}$	$6.550 \times 10^{-3}$	$8.927 \times 10^{-4}$	4.156
$\delta_r$ [%]	-0.03	-0.4	-0.3	-0.2	-0.65
THU [%]	$\pm 0.5$	$\pm 1.0$	$\pm 5.0$	$\pm 0.5$	$\pm 0.73$

**Table 7**

Branching ratios (BRs) of the SM Higgs taking  $M_H = 125.5$  GeV. We compare our numerical estimates with those presented in Ref. [84]. Estimation of the total uncertainty THU+ PU has been done by adding linearly the THU and the total parametric uncertainty (PU) where the latter is obtained by adding the individual PUs in quadrature, see Tables 174, 175, 176, 177, and 178 in Ref. [84].

	$B(H \rightarrow b\bar{b})$	$B(H \rightarrow WW)$	$B(H \rightarrow gg)$	$B(H \rightarrow \tau\tau)$	$B(H \rightarrow c\bar{c})$
This Review	$5.733 \times 10^{-1}$	$2.225 \times 10^{-1}$	$8.190 \times 10^{-2}$	$6.230 \times 10^{-2}$	$2.841 \times 10^{-2}$
Ref. [84]	$5.744 \times 10^{-1}$	$2.219 \times 10^{-1}$	$8.147 \times 10^{-2}$	$6.192 \times 10^{-2}$	$2.852 \times 10^{-2}$
THU+ PU [%]	1.7	2.1	7.2	2.3	6.6
	$B(H \rightarrow ZZ)$	$B(H \rightarrow \gamma\gamma)$	$B(H \rightarrow Z\gamma)$	$B(H \rightarrow \mu\mu)$	$\Gamma_{\text{tot}}$ [MeV]
This Review	$2.758 \times 10^{-2}$	$2.278 \times 10^{-3}$	$1.582 \times 10^{-3}$	$2.159 \times 10^{-4}$	4.129
Ref. [84]	$2.741 \times 10^{-2}$	$2.271 \times 10^{-3}$	$1.576 \times 10^{-3}$	$2.148 \times 10^{-4}$	4.156
THU+ PU [%]	2.1	2.9	6.9	2.4	1.9

- Wrong-sign bottom-quark Yukawa (LHC): a preference of the positive sign at  $\sim 1.5\sigma$

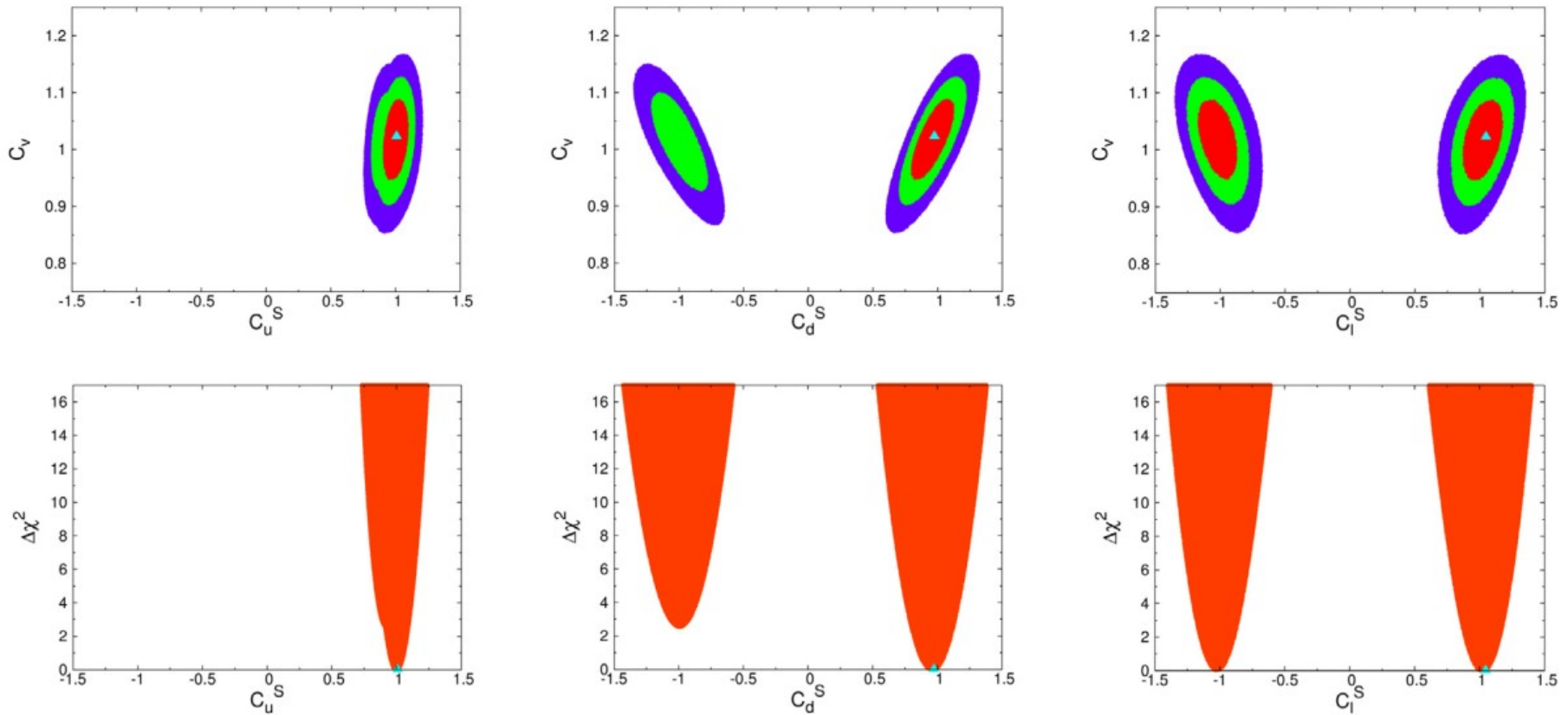


**Fig. 31. CPC4:** (Upper) The confidence-level (CL) regions of the fit by varying  $C_v$ ,  $C_u^S$ ,  $C_d^S$ , and  $C_l^S$ . The contour regions shown are for  $\Delta\chi^2 \leq 2.3$  (red), 5.99 (red+green), and 11.83 (red+green+blue) above the minimum, which correspond to confidence levels of 68.3%, 95%, and 99.7%, respectively. The best-fit points are denoted by triangles. (Lower)  $\Delta\chi^2$  from the minimum versus Yukawa couplings. From Ref. [258].

- Target precisions@FCC-hh (rare decays) FCC-eh is needed to pin down PDF for  $\mu$

**Table S.2** Target precision, at FCC-hh, for the parameters relative to the measurement of various Higgs decays, ratios thereof, and of the Higgs self-coupling. Notice that Lagrangian couplings have a precision that is typically half that of what is shown here, since all rates and branching ratios depend quadratically on the couplings

Observable	Parameter	Precision (stat)	Precision (stat + syst + lumi)
$\mu = \sigma(H) \times B(H \rightarrow \gamma\gamma)$	$\delta\mu/\mu$	0.1%	1.45%
$\mu = \sigma(H) \times B(H \rightarrow \mu\mu)$	$\delta\mu/\mu$	0.28%	1.22%
$\mu = \sigma(H) \times B(H \rightarrow 4\mu)$	$\delta\mu/\mu$	0.18%	1.85%
$\mu = \sigma(H) \times B(H \rightarrow \gamma\mu\mu)$	$\delta\mu/\mu$	0.55%	1.61%
$\mu = \sigma(HH) \times B(H \rightarrow \gamma\gamma)B(H \rightarrow b\bar{b})$	$\delta\lambda/\lambda$	5%	7.0%
$R = B(H \rightarrow \mu\mu)/B(H \rightarrow 4\mu)$	$\delta R/R$	0.33%	1.3%
$R = B(H \rightarrow \gamma\gamma)/B(H \rightarrow 2e2\mu)$	$\delta R/R$	0.17%	0.8%
$R = B(H \rightarrow \gamma\gamma)/B(H \rightarrow 2\mu)$	$\delta R/R$	0.29%	1.38%
$R = B(H \rightarrow \mu\mu\gamma)/B(H \rightarrow \mu\mu)$	$\delta R/R$	0.58%	1.82%
$R = \sigma(t\bar{t}H) \times B(H \rightarrow b\bar{b})/\sigma(t\bar{t}Z) \times B(Z \rightarrow b\bar{b})$	$\delta R/R$	1.05%	1.9%
$B(H \rightarrow \text{invisible})$	$B@95\%CL$	$1 \times 10^{-4}$	$2.5 \times 10^{-4}$

branching ratios. Taking as a given the value of the HZZ coupling (and therefore  $B(H \rightarrow 4\ell)$ ), which will be measured to the few per-mille level by FCC-ee, from the FCC-hh ratios it could be possible to extract the absolute couplings of the Higgs to  $\gamma\gamma$  (0.4%),  $\mu\mu$  (0.7%), and  $Z\gamma$  (0.9%).

- Trilinear Higgs self-coupling (FCC-hh):  $\sim 8(\sim 2)\%$  with 3(30)/ab

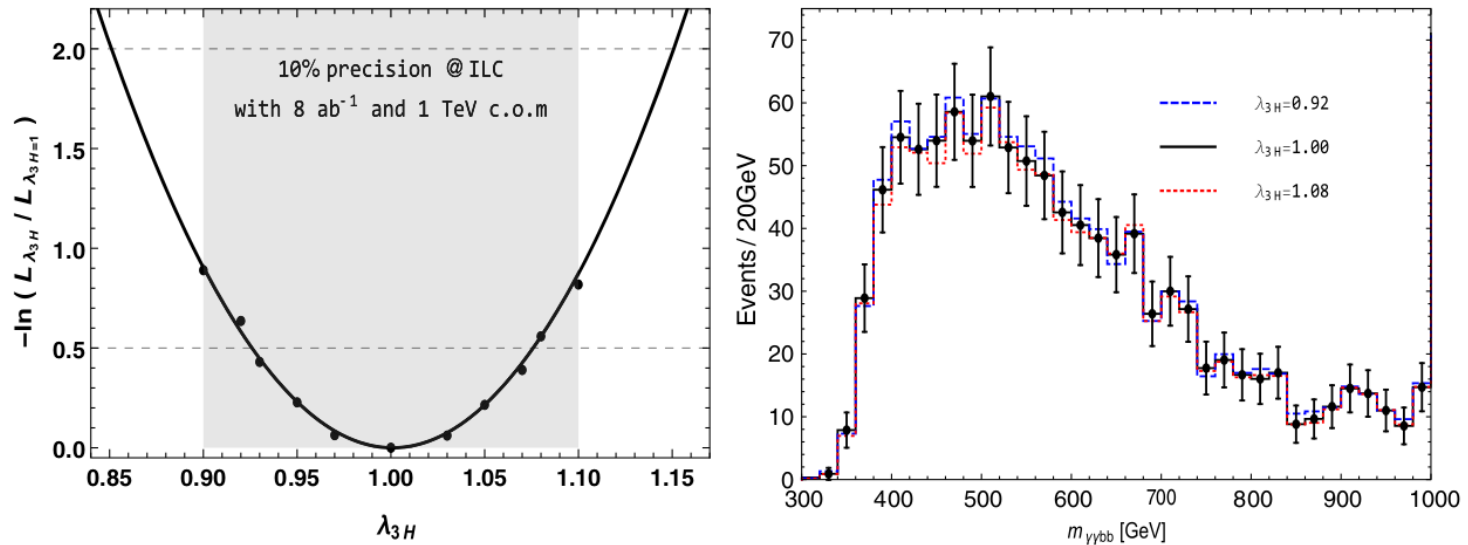


FIG. 3. Left: the relative log likelihood distribution for the nominal value of  $\lambda_{3H} = 1$  at the 100 TeV hadron collider with  $3 \text{ ab}^{-1}$ . The black circles are the values obtained by a likelihood fitting of  $M_{\gamma\gamma bb}$  distributions using  $\text{BDT}_{\text{SM}}$  with the BDT response cut of 0.216. The black solid line shows the result of a polynomial fitting and the thin dashed line at 0.5(2.0) indicates the value corresponding to a  $1\sigma(2\sigma)$  CI. The shaded region shows the  $1\sigma$  CI expected at the ILC at 1 TeV with  $8 \text{ ab}^{-1}$ . Right: the SM  $M_{\gamma\gamma bb}$  distribution (solid line with dots with  $1\sigma$  error bars) and those for  $\lambda_{3H} = 0.92$  and  $1.08$  (dashed lines).

## Measuring the trilinear Higgs boson self-coupling at the 100 TeV hadron collider via multivariate analysis

#5

Jubin Park (Chonnam Natl. U.), Jung Chang (Chonnam Natl. U.), Kingman Cheung (NCTS, Hsinchu and Konkuk U. and Taiwan, Natl. Tsing Hua U.), Jae Sik Lee (Chonnam Natl. U.) (Mar 27, 2020)

Published in: *Phys.Rev.D* 102 (2020) 7, 073002 • e-Print: [2003.12281](https://arxiv.org/abs/2003.12281) [hep-ph]

- The electron Yukawa: H\_run@FCC-ee with  $\sqrt{s} \simeq 129.09 \text{ GeV}$

### *The electron Yukawa coupling*

The measurement of the electron Yukawa coupling is challenging due to the small size of the electron mass. If, for a variety of reasons, the FCC schedule called for a prolongation of the FCC-ee operation, a few additional years spent at centre-of-mass energy in the immediate vicinity of the Higgs boson pole mass,  $\sqrt{s} \simeq 125.09 \text{ GeV}$ , would be an interesting option. At this energy, the resonant production of the Higgs boson in the s channel,  $e^+e^- \rightarrow H$ , has a tree-level cross section of 1.64 fb, reduced to 0.6 fb when initial-state radiation is included, and to 0.3 fb if the centre-of-mass energy spread were equal to the Higgs boson width of 4.2 MeV [81].

A much larger spread, typically of the order of 100 MeV, is expected when the machine parameters are tuned to deliver the maximum luminosity, rendering the resonant Higgs production virtually invisible. The energy spread can be reduced with monochromatisation schemes [82], at the expense of a similar luminosity reduction. It is estimated that  $2(7) \text{ ab}^{-1}$  can be delivered in one year of running at  $\sqrt{s} \simeq 125.09 \text{ GeV}$  with a centre-of-mass energy spread of 6 (10) MeV. From a preliminary cut-and-count study in ten different Higgs decay channels, the resonant Higgs boson production is expected to yield a significance of  $0.4\sigma$  within a year in both scenarios, allowing an upper limit to be set on the electron Yukawa coupling to 2.5 times the SM value. The SM sensitivity can be reached in five years [83].

The FCC-ee therefore offers a unique opportunity to set stringent upper bounds on the electron Yukawa coupling. These bounds are of prime importance when it comes to interpreting electron electric dipole measurements in setting constraints on new physics. The bounds on top CP violating couplings given in Ref. [84], for example, are invalidated if the electron Yukawa coupling is neither fixed to its SM value nor constrained independently.

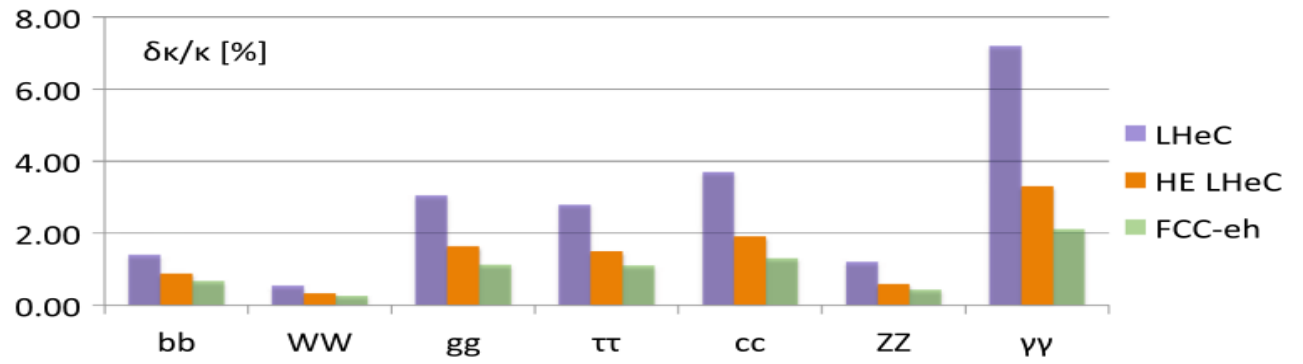
# • Higgs precisions@FCC-ee(repeat) and @FCC-eh

**Table S.1** Precisions determined in the  $\kappa$  framework on the Higgs boson couplings and total decay width, as expected from the FCC-ee data, and compared to those from HL-LHC. All numbers indicate 68% C.L. sensitivities, except for the last line which gives the 95% C.L. sensitivity on the “exotic” branching fraction, accounting for final states that cannot be tagged as SM decays. The fit to the HL-LHC projections alone (first column) requires assumptions: here, the branching ratios into  $c\bar{c}$  and into exotic particles (and those not indicated in the table)

are set to their SM values. The FCC-ee accuracies are subdivided in three categories: the first sub-column gives the results of the fit expected with  $5 \text{ ab}^{-1}$  at 240 GeV, the second sub-column in bold includes the additional  $1.5 \text{ ab}^{-1}$  at  $\sqrt{s} = 365 \text{ GeV}$ , and the last sub-column shows the result of the combined fit with HL-LHC. Similar to the HL-LHC, the fit to the FCC-eh projections alone requires an assumption to be made: here the total width is set to its SM value, but in practice will be taken to be the value measured by the FCC-ee

Collider	HL-LHC	ILC <sub>250</sub>	CLIC <sub>380</sub>	FCC-ee			FCC-eh
Luminosity ( $\text{ab}^{-1}$ )	3	2	0.5	5 @ 240 GeV	+ 1.5 @ 365 GeV	+ HL-LHC	2
Years	25	<b>15</b>	8	<b>3</b>	+ 4	–	20
$\delta\Gamma_{\text{H}}/\Gamma_{\text{H}}$ (%)	<b>SM</b>	3.6	4.7	<b>2.7</b>	<b>1.3</b>	1.1	SM
$\delta g_{\text{HZZ}}/g_{\text{HZZ}}$ (%)	1.5	0.30	0.60	<b>0.2</b>	<b>0.17</b>	0.16	0.43
$\delta g_{\text{HWW}}/g_{\text{HWW}}$ (%)	1.7	1.7	1.0	1.3	<b>0.43</b>	0.40	0.26
$\delta g_{\text{Hbb}}/g_{\text{Hbb}}$ (%)	3.7	1.7	2.1	1.3	<b>0.61</b>	0.56	0.74
$\delta g_{\text{Hcc}}/g_{\text{Hcc}}$ (%)	<b>SM</b>	2.3	4.4	1.7	<b>1.21</b>	1.18	1.35
$\delta g_{\text{Hgg}}/g_{\text{Hgg}}$ (%)	2.5	2.2	2.6	1.6	<b>1.01</b>	<b>0.90</b>	1.17
$\delta g_{\text{H}\tau\tau}/g_{\text{H}\tau\tau}$ (%)	1.9	1.9	3.1	1.4	<b>0.74</b>	0.67	1.10
$\delta g_{\text{H}\mu\mu}/g_{\text{H}\mu\mu}$ (%)	4.3	14.1	n.a.	10.1	<b>9.0</b>	3.8	n.a.
$\delta g_{\text{H}\gamma\gamma}/g_{\text{H}\gamma\gamma}$ (%)	1.8	6.4	n.a.	4.8	<b>3.9</b>	<b>1.3</b>	2.3
$\delta g_{\text{Ht}}/g_{\text{Ht}}$ (%)	3.4	–	–	–	–	3.1	1.7
$\text{BR}_{\text{EXO}}$ (%)	<b>SM</b>	< 1.8	< 3.0	< 1.2	< <b>1.0</b>	< 1.0	n.a.

**Fig. 4.12** Determination of the  $\kappa$  scaling parameter uncertainties, from a joint SM fit of CC and NC signal strength results for the FCC-eh (green,  $2 \text{ ab}^{-1}$ ), the HE LHeC (brown,  $2 \text{ ab}^{-1}$ ) and LHeC (blue,  $1 \text{ ab}^{-1}$ )



#### 4.5.2 Determination of Higgs couplings

The amplitude of the subprocess,  $VV \rightarrow H \rightarrow XX$  ( $X = b, W, g, \tau, c, Z, \gamma$ ) involves a coupling to the vector boson  $V$ , scaling as  $\kappa_V$ , and the coupling to the decay particle  $X$ , proportional to  $\kappa_X$ , modulated by a  $\kappa$  dependent factor due to the total decay width. This leads to the following scaling of the signal strength

$$\mu_X^V = \kappa_V^2 \cdot \kappa_X^2 \cdot \frac{1}{\sum_j \kappa_j^2 \text{BR}_j}, \quad (4.1)$$

which is the ratio of the experimental to the theoretical cross sections, expected to be 1 in the SM. Measurements of this quantity at the LHC are currently accurate to  $\mathcal{O}(20)\%$  and will reach the  $\mathcal{O}(5)\%$  level at the HL-LHC. With the joint CC and NC measurements of the various decays, considering the seven most abundant ones illustrated in Fig. 4.11, one constrains with the above equation the seven  $\kappa_X$  parameters. The joint measurement of NC and CC Higgs decays provides 9 constraints on  $\kappa_W$  and 9 on  $\kappa_Z$  together with 2 each for the five other decay channels considered. Since the dominating channel of  $H \rightarrow b\bar{b}$  is precisely determined, there follows a strikingly precise determination of the  $\kappa$  values, to about or below one percent, as is shown in Fig. 4.12. A feature worth noting is the “transfer” of precision in signal strength from the  $\mu_b$  in the CC channel to  $\kappa_W$ . This overall level of precision may as well be used to constrain EFT parameters, a task beyond the standalone FCC-eh analysis presented here.

A fundamental quantity to be accessed, linking the two heaviest SM elementary particles, is the  $t\bar{t}H$  coupling, and its associated CP phase  $\zeta_t$ , expected to vanish in the SM. An update of the LHCeC analysis documented in Ref. [97] shows that FCC-eh could achieve a precision of 1.9% in the determination of  $\zeta_t$ .

backgrounds such as single top and  $W$  photoproduction. The resulting uncertainty on the invisible Higgs branching ratio is estimated to be 1.2%.